Research article

The potential of industrial waste: using foundry sand with fly ash and electric arc furnace slag for geopolymer brick production

Suchanya Apithanyasai [a], Nuta Supakata [b,c,d,*], Seksan Papong [e]

[a] International Program in Hazardous Substance and Environmental Management, Graduate School, Chulalongkorn University, Bangkok, Thailand
[b] Department of Environmental Science, Faculty of Science, Chulalongkorn University, Bangkok, Thailand
[c] Research Program: Municipal Solid Waste and Hazardous Waste Management, Center of Excellence on Hazardous Substance Management, Thailand
[d] Waste Utilization and Ecological Risk Assessment Research Group, The Ratchadaphiseksomphot Endowment Fund, Chulalongkorn University, Thailand
[e] Department of Life Cycle Assessment Laboratory, National Metal and Materials Technology Center, MTEC, Bangkok 12120, Thailand

ARTICLE INFO

ABSTRACT

The purpose of this study was to investigate the best ratio of waste foundry sand (WFS), fly ash (FA), and electric arc furnace slag (EAF slag) for the production of geopolymer bricks. In this research study, WFS, FA, and EAF slag were mixed at the ratio of 70:30:0, 60:30:10, 50:30:20, and 40:30:30 with 8M sodium hydroxide (NaOH) and 98% purity sodium silicate (Na_2SiO_3) with a ratio of Na_2SiO_3/8M NaOH = 2.5. The mixtures were compacted in 5 cm × 5 cm x 5 cm molds and cured at an ambient temperature for 28 days. Then, their compressive strength was analyzed. The results showed that the geopolymer bricks with the highest compressive strength were those mixed at the 40:30:30 ratio, with a compressive strength of 25.76 MPa. The strongest bricks were also analyzed using the leaching test to ensure the production involved non-hazardous materials. To compare the environmental impacts of geopolymer bricks and concrete bricks, their effects on climate change, ozone depletion, terrestrial acidification, human toxicity, terrestrial ecotoxicity, and fossil fuel depletion were examined from cradle to grave using SimaPro 8.0.5.13 software. The results of the life cycle assessment (LCA) from cradle to grave showed that the environmental impact of geopolymer brick production was lower in every aspect than that of concrete production. Therefore, geopolymer brick production can reduce environmental impact and can be a value-added use for industrial waste.

1. Introduction

Increasing amounts of industrial by-products and waste materials, as well as a lack of landfill space, will become even greater environmental issues. Managing solid waste by-products and materials by repurposing them has therefore become an attractive alternative form of disposal (Siddique and Singh, 2011).

Waste foundry sand (WFS) is a by-product of both ferrous (iron and steel) and nonferrous (copper, aluminum, and brass metal) castings production, and WFS is used for molding and casting operations with high-quality silica sand (Siddique et al., 2010; Siddique and Noumowe, 2008). In 2015, approximately 100,000 tons of WFS were disposed of in Thai landfills (HSM, 2015). WFS can be made into many alternative forms that could be added to concrete, asphalt, and pavement and used in the construction of highway bases, retaining structures, and landfill liners (Gürkan et al., 2018; Siddique et al., 2010). Because no one has yet

studied the production of geopolymer brick from WFS, it may be possible to produce pavement brick from WFS with geopolymerization technique.

Geopolymer is created from the chemical reaction (geopolymerization) between aluminosilicate materials, which are industrial by-products, and alkaline activators. Alkaline activators are commonly a mix of sodium or potassium hydroxide and liquid sodium or calcium silicate (Hadi et al., 2018). Two phases of geopolymer gel network formation occur when aluminosilicate materials react with the alkaline activators, producing sodium aluminosilicate hydrate gel (NASH) and calcium silicate hydrate (CSH) (Li et al., 2010). These two gel networks have different functions in the geopolymer production. NASH is a tetrahedral network of SiO_4 and AlO_4 with shared oxygen atoms, creating a three-dimensional structure. CSH is the major binding phase in alkali-activated materials, and it is like a polymer. Thus, CSH can enhance the compressive strength of geopolymers. WFS contains high amounts of silica and lacks alumina and calcium. It is therefore necessary

---

to add several waste materials that contain alumina and calcium to form geopolymers and to enhance their compressive strength.

Fly ash (FA) is a by-product of coal-fired electric power stations. Approximately 10,000 tons of coal ash has been produced per day by the Electricity Generating Authority of Thailand (EGAT) in Mae Moh, Lumpang Province, resulting in approximately six thousand tons of FA, an amount that continuously increases. SiO_2, Al_2O_3, and Fe_2O_3 are the major parts (50–70% by weight) of Class C lignite FA coming from EGAT. FA can be used as a partial substitute for soil aggregate for groundwork construction, groundwork reparation, and the construction of pavement layers (EGAT, 2018). Furthermore, if the chemical composition of FA has a high percentage of silica (60–65%), alumina (25–30%), and magnetite (6–15%), it is possible to use FA as a geopolymer binder to form NASH (Arulrajah et al., 2016; Fang et al., 2018; Phummiphan et al., 2018). FA could also create new products for use in the manufacture of cement, building-material concrete, and concrete admixtures.

Electric arc furnace slag (EAF slag), the residue of the production of molten steel from scrap metal in the EAF is discharged and disposed of in landfills when the melting of the EAF section is completed (Apithanyasai et al., 2018); approximately one million tons have been added to Thai landfills (HSM, 2015). Referred to Yi et al. (2012), EAF slag waste can be managed by recycling as raw material in the construction and building work with environment-friendliness such as aggregate, brick, ceramic tile, and cement. Their research shows that EAF slag can enhance the compressive strength property of geopolymer because of CSH structures, forming by calcium oxide (CaO) content in EAF slag (Zhang et al., 2016).

In this study, FA and EAF were used as raw materials to develop a geopolymer binder to produce bricks; this use of FA and EAF could be a low–environmental impact method of waste management. WFS was mixed with different combinations of FA- and EAF-based geopolymers to enhance the strength properties of WFS bricks for pavement applications. This study examined the characteristics of these geopolymer bricks, including their compressive strength, microstructure, mineralogical phases, and infrared spectra. The geopolymer bricks with the highest compressive strength were then tested for the leaching of heavy metals, according to the toxicity characteristic leaching procedure (TCLP) method. Life cycle assessment (LCA) was used to identify the environmental impact of the bricks. The results of this study can be used to create environmentally friendly solutions for industrial waste management.

2. Materials and methods

2.1. Raw materials

WFS was obtained from Kitagawa Co., Ltd. (Chonburi Province, Thailand). FA was obtained from the Electricity Generating Authority of Thailand (EGAT) (Mae Moh, Lampang Province, Thailand). EAF slag was collected from the iron and steel industry at Siam Yamato Steel Co., Ltd. in Rayong province, Thailand.

Before their use, WFS and EAF were crushed in a jaw crusher, roll crusher, and ball mill, and the particles were passed through sieve No. 200 with a diameter of 75 μm to ensure the particles were the correct size by vibrating screen. Because of its smaller size, FA was passed through sieve No. 200 without crushing. Then, the characteristics of WFS, EAF, and FA were analyzed by using methods mentioned in Apithanyasai et al. (2018).

2.2. Preparation of alkaline solution

The alkaline solution is a mixture of 8 M sodium hydroxide (NaOH) and 98% purity sodium silicate (Na_2SiO_3) with a ratio of Na_2SiO_3/8 M NaOH = 2.5 (Arulrajah et al., 2016). The alkaline solution was cooled at room temperature for 24 h to decrease gas bubbles in the liquid before use.

2.3. Preparation of geopolymer bricks

The proportion of FA in the total mix was fixed at 30% (Phummiphan et al., 2018), while the EAF contents were varied to partially substitute WFS from 0% to 30% (Fang et al., 2018), as shown in Table 1.

The geopolymer proportions shown in Table 1 were dry mixed for two minutes to ensure homogeneity, and then the alkaline activator was added by shaking during three minutes of mixing. The weight ratio of alkaline solution to mixed powder was set at 0.4 for all treatments. The mixtures were compacted in a cube sample (5 cm × 5 cm × 5 cm), according to standard test method ASTM C 109/C 109M (2014). Air bubbles were then removed from the mixtures using a vibration machine for five minutes. The compact samples were de-molded after 24 h, immediately wrapped with plastic sheets, and cured at room temperature for 28 days. Then, the compressive strength of the geopolymer bricks was examined according to standard test method ASTM C 109/C 109M (2014). The physical and chemical properties of the geopolymer bricks were analyzed using methods mentioned in Apithanyasai et al. (2018).

2.4. Leaching of heavy metals

Using the TCLP method, the samples were crushed and were sieved using a 9.5 mm standard sieve. Then, the TCLP extraction fluid was examined by measuring the pH of the test sample (USEPA, 1992). The samples were then extracted using the selected extraction fluid. The samples had a solid-to-extraction fluid ratio of 1:20 and were placed in centrifuge bottles. The samples were rotated at 30 ± 2 rpm in a rotator-mixer (Multi RS-60, BIOSAN) for 18 ± 2 h. The extract was preserved by adding nitric acid until its pH was <2. The extract was separated from the solid phase by filtering it through a 0.7 μm glass fiber filter. The extracted samples were analyzed for heavy metals using inductively coupled plasma mass spectrometry.

2.5. Life cycle assessment (LCA)

The goal of LCA in this study was to compare the environmental life cycle impact of geopolymer bricks made of WFS, FA, and EAF with that of concrete bricks. The scope of this study was from cradle to grave, covering the period from materials acquisition to the production of geopolymer bricks to the disposal of construction and demolition waste in landfills. The functional unit was defined as the geopolymer bricks needed to fill one square meter of pavement.

The life cycle inventory data on the optimal ratio of materials to make geopolymer bricks, which was 40% WFS, 30% FA, and 30% EAF slag, was determined by a lab-scale experiment on a five-cubic centimeter sample. Life cycle inventory shows the material and energy flow (input and output) at every stage of the life cycle of geopolymer bricks, from raw materials acquisition to disposal. This process can be divided into two parts: 1) LCA of raw materials acquired to create geopolymer bricks with a compressive strength of 25 MPa, as shown in Table 2, and 2) LCA of concrete bricks with a compressive strength of 25 MPa strength whose data is available in the ecoinvent database of SimaPro*. These concrete bricks included Quebec concrete (CA-QC) composed of cement (237 Kg), water (164 Kg), gravel (950 Kg), sand (940 Kg), and FA (18 Kg), and North American concrete (RoW) composed of cement (204 Kg), water (160 Kg), gravel (1009 Kg), sand (925 Kg), and FA (36 Kg), as shown in Table 3. There are seven steps in the production of geopolymer bricks: diesel production, alkaline solution processes, material preparation, geopolymer processes, transportation, utilization, and disposal of materials at the landfill, as shown in Figure 1.

The life cycle assessment study was carried out using SimaPro 8.0.5.13 software from the National Metal and Materials Technology Center. The results were expressed in six categories of impact, which were climate change, ozone depletion, terrestrial acidification, human toxicity, terrestrial ecotoxicity, and fossil fuel depletion.
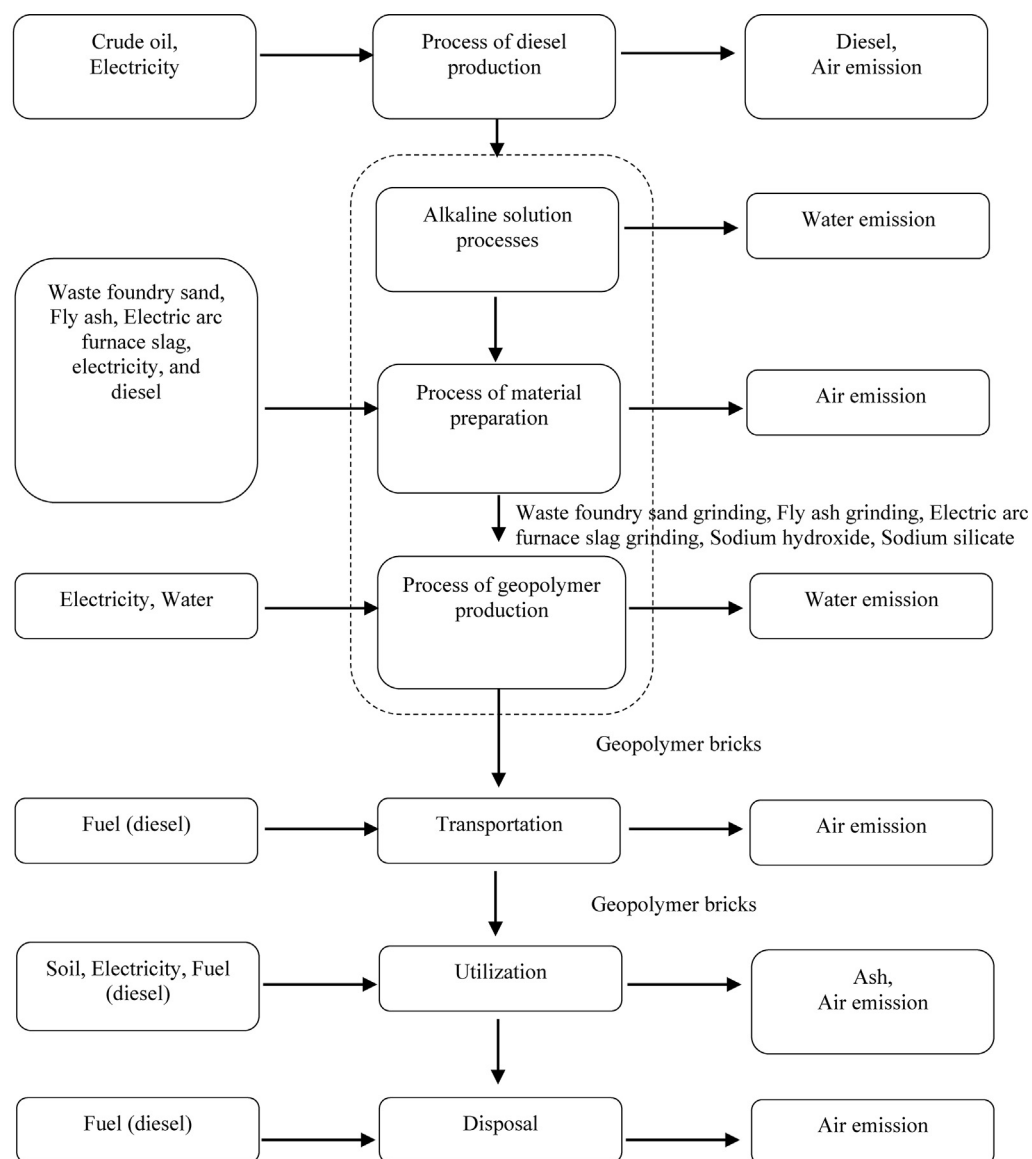
Table 1. *Geopolymer formulations.*

Name	WFS (wt. %)	FA (wt. %)	EAF (wt. %)
WFS70	70	30	0
WFS60	60	30	10
WFS50	50	30	20
WFS40	40	30	30

Table 2. *The inventory data of each life cycle stage of 1 m^2 geopolymer brick.*

Item	Unit	The inventory data					
		Alkaline solution process	Material preparation process	Geopolymer processes	Transportation process	Utilization process	Disposal
Inputs							
WFS	kg	-	28.8	-	-	-	-
FA	kg	-	21.6	-	-	-	-
EAF slag	kg	-	21.6	-	-	-	-
NaOH	kg	2.04	-	-	-	-	-
Na$_2$SiO$_3$	kg	20.80	-	-	-	-	-
Diesel	kg	-	5.81	-	0.85	-	0.85
Brick	unit	-	-	-	400	400	-
Sand	kg	-	-	-	-	40	-
Water	l	6.36	-	15	-	10	-
Electricity	kWh	5.1	3.91	0.16	-	-	-
Air pollution							
NOx	kg	-	1.03×10^{-4}	-	1.49×10^{-5}	-	1.49×10^{-5}
CO	kg	-	1.32×10^{-5}	-	1.92×10^{-6}	-	1.92×10^{-6}
NMVOC	kg	-	5.00×10^{-6}	-	7.28×10^{-7}	-	7.28×10^{-7}
SOx	kg	-	9.41×10^{-6}	-	1.37×10^{-6}	-	1.37×10^{-6}
TSP	kg	-	4.00×10^{-6}	-	5.83×10^{-7}	-	5.83×10^{-7}
PM10	kg	-	4.00×10^{-6}	-	5.83×10^{-7}	-	5.83×10^{-7}
PM2.5	kg	-	4.00×10^{-6}	-	5.83×10^{-7}	-	5.83×10^{-7}
Pb	kg	-	1.60×10^{-11}	-	2.33×10^{-12}	-	2.33×10^{-12}
Cd	kg	-	1.20×10^{-12}	-	1.75×10^{-13}	-	1.75×10^{-13}
Hg	kg	-	2.40×10^{-11}	-	3.50×10^{-12}	-	3.50×10^{-12}
As	kg	-	6.00×10^{-12}	-	8.74×10^{-13}	-	8.74×10^{-13}
Cr	kg	-	4.00×10^{-11}	-	5.83×10^{-12}	-	5.83×10^{-12}
Cu	kg	-	4.40×10^{-11}	-	6.41×10^{-12}	-	6.41×10^{-12}
Ni	kg	-	1.60×10^{-12}	-	2.33×10^{-13}	-	2.33×10^{-13}
Se	kg	-	2.20×10^{-11}	-	3.20×10^{-12}	-	3.20×10^{-12}
Zn	kg	-	5.80×10^{-9}	-	8.45×10^{-10}	-	8.45×10^{-10}
Benzo(a)pyrene	kg	-	3.80×10^{-10}	-	5.54×10^{-11}	-	5.54×10^{-11}
Benzo(b)floranthene	kg	-	3.00×10^{-9}	-	4.37×10^{-10}	-	4.37×10^{-10}
Benzo(k)fluoranthene	kg	-	3.40×10^{-10}	-	4.95×10^{-11}	-	4.95×10^{-11}
Indeno(1,2,3-cd)pyrene	kg	-	3.00×10^{-10}	-	4.37×10^{-11}	-	4.37×10^{-11}

Table 3. *The inventory data of 1 m^3 geopolymer brick and 1 m^3 concrete bricks.*

Item	Unit	The inventory data		
		Geopolymer brick	Quebec concrete	North America concrete
WFS	kg	567	0	0
FA	kg	432	18	36
EAF	kg	432	0	0
NaOH	kg	41	0	0
Na$_2$SiO$_3$	kg	416	0	0
Cement	kg	0	237	204
Gravel	kg	0	950	1009
Sand	kg	0	950	925
Water	l	427	164	169

```
┌─────────────────┐        ┌─────────────────┐        ┌─────────────────┐
│ Crude oil,      │──────▶ │ Process of diesel│──────▶ │ Diesel,         │
│ Electricity     │        │ production       │        │ Air emission    │
└─────────────────┘        └─────────────────┘        └─────────────────┘
```

Figure 1 flow diagram:

- Crude oil, Electricity → Process of diesel production → Diesel, Air emission
- Alkaline solution processes → Water emission
- Waste foundry sand, Fly ash, Electric arc furnace slag, electricity, and diesel → Process of material preparation → Air emission
- Waste foundry sand grinding, Fly ash grinding, Electric arc furnace slag grinding, Sodium hydroxide, Sodium silicate
- Electricity, Water → Process of geopolymer production → Water emission
- Geopolymer bricks
- Fuel (diesel) → Transportation → Air emission
- Geopolymer bricks
- Soil, Electricity, Fuel (diesel) → Utilization → Ash, Air emission
- Fuel (diesel) → Disposal → Air emission

*Air emission = CO_2, CO, NO_X, SO_2, NMVOC, PM, NH_3, Benzo(a)pyrene, Benzo(k)fluoranthene, Benzo(b)fluoranthene

Figure 1. Life cycle inventory of geopolymer bricks.

3. Results and discussion

3.1. Characteristics of waste foundry sand (WFS), fly ash (FA), and electric arc furnace slag (EAF slag)

3.1.1. Chemical composition

The chemical compositions of WFS, FA, and EAF slag analyzed by using an X-ray fluorescence spectrometer (Bruker model S8 Tiger) were shown in Table 4. The results found that the major component of WFS was SiO_2 (83.6 %), and Al_2O_3 (2.91 %) and CaO (0.417%) were its minor components. FA had major components, including SiO_2 (32.9%), Al_2O_3 (17.8%), and CaO (18.8%), while Fe_2O_3 (12.4 %), CaO (19.4%), and Fe_2O_3 (32.7%) were the major components of EAF slag.

3.1.2. Particle sizes

The results of particle sizes of WFS, FA, and EAF analyzed by a laser particle distribution analyzer (Malvern Mastersizer 3000) showed their average particle sizes (d_{50}) were 66.9, 11.2, and 127.0 μm, respectively, as shown in Figure 2.

3.1.3. The mineralogical phase

The mineralogical phases of WFS, FA, and EAF were analyzed by XRD (D8 Discover). The results showed that only the major crystalline phase of WFS was quartz (SiO_2). The major mineralogical phases of FA were quartz (SiO_2), potassium aluminum silicate ($K(AlSi_2O_6)$) and lime (CaO), and its minor mineralogical phases were maghemite-C (syn-Fe_2O_3), hematite (alpha-Fe_2O_3), and magnetite (syn-Fe_3O_4). EAF's major mineralogical phase was Wüstite wuestite (FeO), and its minor phases were fayalite (Fe_2+2SiO_4) and bredigite (syn-$Ca_{14}Mg_2(SiO_4)_8$), as shown in Figure 3.

3.1.4. Microstructures of the raw materials

The microstructures of WFS, FA, and EAF were identified using a scanning electron microscope (Jeol JSM-6480LV). As shown in Figure 4,

Table 4. *The chemical composition of waste foundry sand (WFS), fly ash (FA), and electric arc furnace slag (EAF slag).*

Oxides	Content (wt. %)		
	WFS	FA	EAF
SiO_2	83.6	32.9	11.8
Al_2O_3	2.91	17.8	5.83
CaO	0.417	18.8	19.4
Fe_2O_3	1.71	12.4	32.7
SO_3	628 (ppm)	4.53	0.205
MgO	0.994	2.33	3.63
K_2O	0.526	2.18	291 (ppm)
Na_2O	0.368	1.95	519 (ppm)
TiO_2	727 (ppm)	0.418	0.528
P_2O_5	231 (ppm)	0.232	0.311
Cl	156 (ppm)	-	244 (ppm)
BaO	0.0 (ppm)	0.118	0.191
SrO	25.2 (ppm)	0.109	531 (ppm)
MnO	250 (ppm)	922 (ppm)	5.33
As_2O_3	-	285 (ppm)	-
V_2O_5	0.0 (ppm)	268 (ppm)	0.121
Cr_2O_3	0.124	172 (ppm)	2.28
ZnO	443 (ppm)	163 (ppm)	70.6 (ppm)
Nb_2O_5	-	-	225 (ppm)
ZrO_2	106 (ppm)	138 (ppm)	198 (ppm)
Rb_2O	22.6 (ppm)	121 (ppm)	-
NiO	152 (ppm)	90.4 (ppm)	0.0 (ppm)
CuO	52.0 (ppm)	82.4 (ppm)	113 (ppm)
CoO	0.0 (ppm)	0.0 (ppm)	0.0 (ppm)
Ag	-	0.0 (ppm)	-
Au	0.0 (ppm)	0.0 (ppm)	0.0 (ppm)
Hg	0.0 (ppm)	0.0 (ppm)	0.0 (ppm)
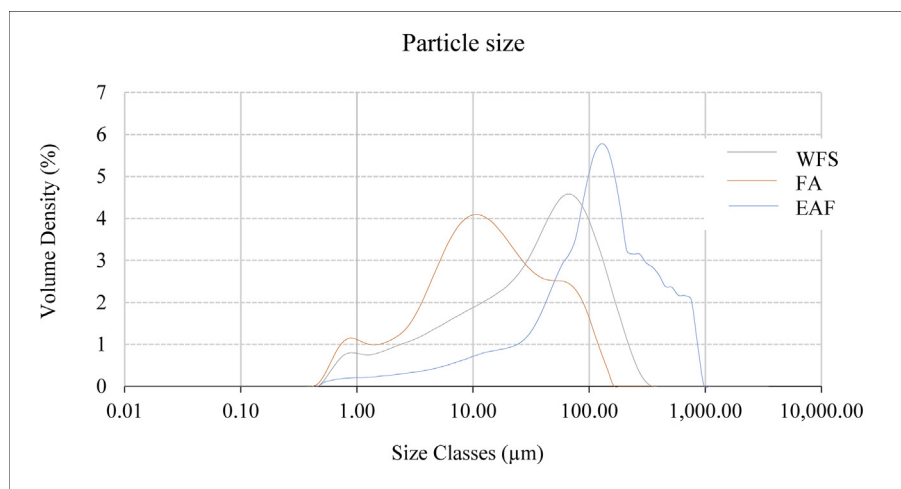
Figure 2. *The particle size of the raw materials.*

the particle shapes of WFS and EAF looked similar to each other, with a stone-shape morphology and few pores, while the FA particles had spherical shapes.

3.2. Characteristics of geopolymer bricks made from waste foundry sand (WFS), fly ash (FA), and electric arc furnace slag (EAF slag)

The cube specimens of the geopolymer bricks had a black color and smooth surfaces, as shown in Figure 5. The specimens were tested to determine their compressive strength (ASTM C 109/C 109M, 2014) using an AMSLER automatic hydraulic testing machine with a maximum capacity of 20 tons. After the testing with the hydraulic machine, parts of the fractured specimen were chosen and crushed by hand with a metallic mortar and pestle. The ground powders were characterized by XRD (D8 Discover), Fourier transform infrared (Perkin Elmer, Spectrum One), and scanning electron microscopy (Jeol JSM-6480LV).

3.2.1. Compressive strength of geopolymer bricks

The compressive strength of the geopolymer bricks after curing for 28 days is shown in Figure 6. The compressive strengths of WFS70, WFS60,

Figure 3. *X-ray diffractometer (XRD) pattern of raw materials.*
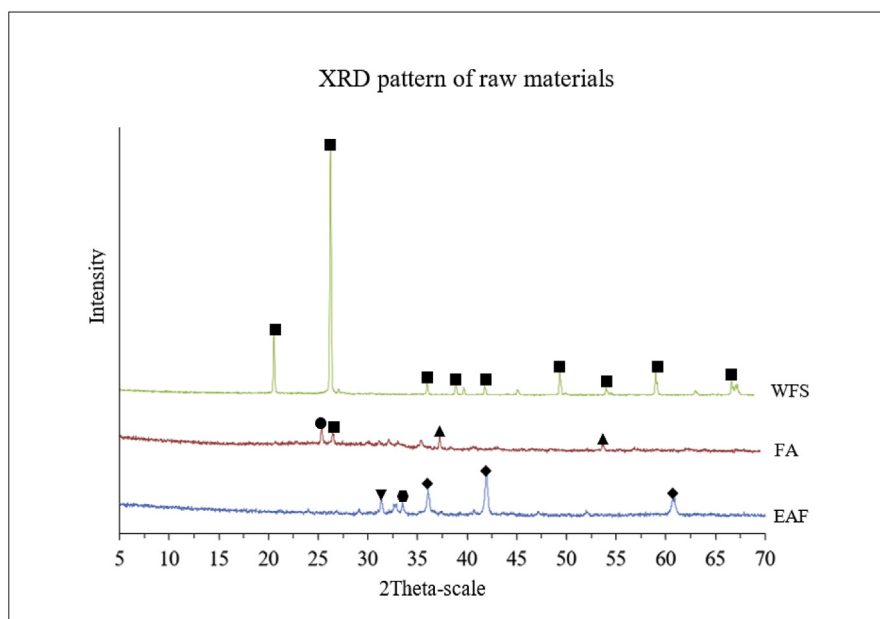
Quartz (SiO_2)   Potassium Aluminum Silicate ($K(AlSi_2O_6)$)   Lime (CaO)
Wuestite (FeO)   Fayalite (Fe_2+2SiO_4)   Bredigite (syn-$Ca_{14}Mg_2(SiO_4)_8$)
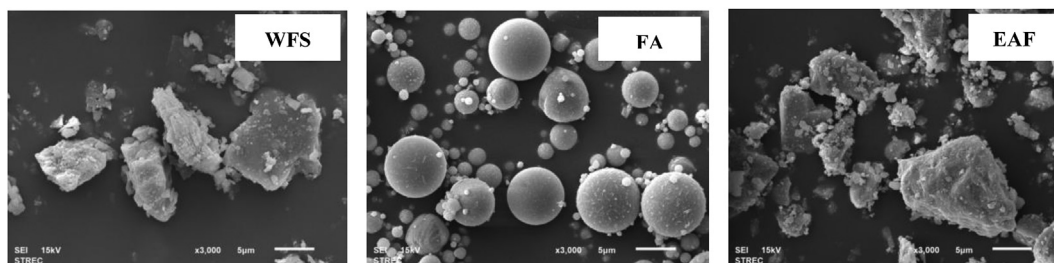

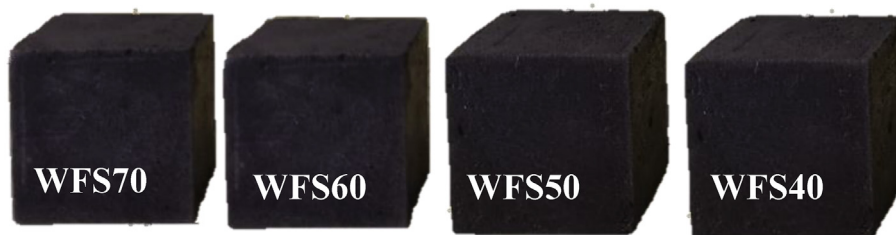**Figure 4.** *Microstructures of WFS, FA, and EAF.*

Figure 5. *The appearance of the geopolymer bricks.*

WFS50, and WFS40 are 18.93, 20.13, 22.92 and 25.76 MPa, respectively; WFS40 obtained the highest compressive strength, and the compressive strength of both WFS50 and WFS40 were above the requirements of paving bricks (ASTM C902 1995) type II (>20.7 MPa).

As expected, decreased WFS content, which ranged from 70% to 40%, resulted in increased compressive strength. The increment in compressive strength with lower WFS content could be attributed to the decrement of the silicate content and the higher Ca and Al contents in the geopolymer mixture. According to Davidovits and Orlinski (1988), the ratio of SiO_2 to Al_2O_3 in geopolymer gel should be in the range of 3.3–4.5. In this experiment, the decrement of WFS from 70% to 40% decreased the ratio of SiO_2 to Al_2O_3 from 7.2 to 3.6, which falls into the range for geopolymer gel. This affected the production of CSH gel because the reactivity of SiO_2 is higher than that of Al_2O_3 (Huseien et al., 2018). In addition, increasing the Al and Ca content by adding FA at a proportion of 30% enhanced the production of CSH gel.

Adding EAF also increased the content of Ca, causing a higher rate of formation of CSH gel, which reduces the porosity and condenses the microstructure of the geopolymer mixture (Fang et al., 2018). It can be concluded that increased EAF content, with its high CaO levels, caused greater formation of CSH gel, which enhanced the bricks' compressive strength.
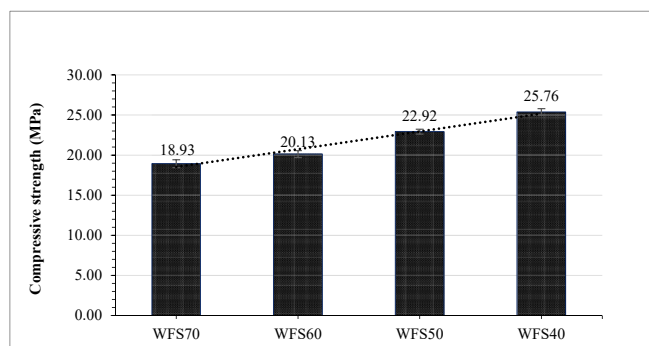
Figure 6. *The compressive strength of geopolymer bricks.*

The compressive strength of geopolymer bricks at 28 days was found to be the highest (25.76 MPa) with 30% EAF content and 30% FA content.

3.2.2. Mineralogical phases of geopolymer bricks

The mineralogical phases of geopolymer bricks after curing for 28 days at an ambient temperature were identified using XRD analysis. The geopolymers that formed after the alkaline-activation processes were mainly amorphous but some were semi-crystalline. Semi-crystalline phases were observed in geopolymer bricks because new phases formed during the alkali-activation process, and crystalline phases were observed because of unreacted raw materials, as shown in Figure 7.

The XRD patterns shown in Figure 7 illustrate that the major phases of the geopolymer brick samples were semi-crystalline CSH phases (WFS60, WFS50, and WFS40) due to the increasing amount of CaO in EAF slag at 10%, 20%, and 30 % in WFS60, WFS50, and WFS40, respectively. This semi-crystalline phase positively affects the formation of amorphous geopolymer and enhances the bricks' compressive strength. CSH, which consists of a three-dimensional amorphous aluminosilicate network called a geopolymer gel, had peaks at $(2\theta) = 37.0^\circ$, 42.7°, and 55.3°.

Quartz mineral (SiO_2) was a major crystalline phase of WFS70, and CSH was not observed due to the absence of CaO content in EAF slag and the high amount of SiO_2 in WFS, which led to unreacted geopolymer gel; however, the SiO_2 phase occurred in all brick samples and had unreacted phases after the alkaline-activation process in geopolymer brick preparation.

3.2.3. Microstructure of geopolymer bricks

SEM images of original FA and FA after reaction with an alkaline solution are shown in Figure 8 (a) and (b), respectively. The surface of original FA was smooth, but when the mineral melted during coal combustion, fly ash particles were formed with a crystalline phase at the core and a glassy phase of silica and alumina at the surface layer (Chindaprasirt and Rattanasak, 2017), as shown in Figure 8 (b). This glassy phase had an influence on the geopolymerization because of the high solubility of the alkaline solution. When FA particles interacted with the alkaline solutions, the surface of FA was attacked, and the reaction products of CSH and aluminosilicate (geopolymer) compounds formed around the FA particles shown in the XRD patterns.

The microstructure of geopolymer bricks with different ratios of raw materials (WFS70, WFS60, WFS50, and WFS 40) after curing at an ambient temperature for 28 days were characterized by SEM, and the images are shown in Figure 9. The SEM investigation can help to better understand the morphologies of the formed geopolymer composites.

SEM images in Figure 9 shows that the morphology of the formation of the new geopolymer phase was entirely different compared with the starting materials (Figure 4). The alkaline activation of the WFS and FA led to dissolution of the aluminosilicate materials, which produced a

tetrahedral polymer that is connected with others forming three-dimensional chains (Zawrah et al., 2016). The SEM images show that geopolymer gels are exhibited in the whole sample of the new geopolymer phase, of which the microstructure was uniform with some crystals in the gel matrix.

As shown in the SEM micrographs in Figure 9 (a), the uncompleted geopolymerization reactions in the specimens caused the non-reaction of raw materials exhibited in the WFS70 specimen confirmed by the XRD analysis in Figure 7. The SEM micrographs for the WFS60, WFS50, and WFS40 specimens in Figures 9 (b), (c), and (d) show that these samples containing 10%, 20%, and 30% EAF slag, respectively, were more compact and massive and less porous than WFS70, which had 0% EAF slag. Moreover, the SEM shows that some large particles entered the matrix and partially reacted during the alkaline activation process, which describes that the distribution of particle size has an influence on the geopolymerization completion. During the geopolymerization process, particles with smaller size completely reacted and dissolved, while particles with larger size partially reacted. Referred to Zhang et al. (2016), the particle size and specific surface area of the beginning raw materials play the major role on the reactivity and on the properties of derived geopolymer due to their influence on the extent and rate of geopolymerization reaction.

The formation of additional CSH with fibrous structure morphology in the geopolymer gel network shown by the SEM micrograph enhanced the density of these specimens microstructure. Consequently, the other calcium-rich semi-crystalline components were formed by the geopolymer reaction increased by the proportion of EAF slag, which could be the improved structure and greater strength of the geopolymer (Zhang et al., 2014).

3.2.4. Leaching of heavy metals from WFS40

The geopolymer brick WFS40, which had the highest compressive strength, was tested for different types of heavy metals (As, Cr, Cu, Mn, Pb and Zn) according to the TCLP method with select extraction fluid #2 pH $= 2.88 \pm 0.05$ (prepared by diluting 5.7 ml of CH_3COOH with water to 1 L), and the results are shown in Table 5. The test results showed that heavy metal concentrations in geopolymer bricks are lower than TCLP limits. Because the leaching concentrations of heavy metals in the TCLP extracts are lower than TCLP limits, this brick can be classified as non-hazardous waste.

3.3. Life cycle assessment (LCA)

The LCA of geopolymer bricks made of 40% WFS, 30% FA, and 30% EAF slag, which had a compressive strength of 25 MPa, is presented in this section. The LCA was used to determine the life-cycle impact of these bricks from cradle to grave. The impact categories included climate change, ozone depletion, terrestrial acidification, human toxicity, terrestrial ecotoxicity, and fossil fuel depletion.

3.3.1. Environmental impact life cycle assessment (LCA) categories of geopolymer bricks

The environmental impact of the processes of material acquisition, production, utilization, and disposing of the geopolymer bricks made from 40% WFS, 30% FA, and 30% EAF was analyzed, and the distribution of the environmental impact of each life cycle stage is presented in Figure 10. The results can be explained as follows.

The main factors affecting climate change were the alkaline solution preparation process and the material preparation process at 40.47% and 43.88%, respectively. The electricity used by the fume hood equipment and the grinding and sieving machines as well as the air pollutants from transporting raw materials contributed to this impact.

The main factor involved in ozone depletion was alkaline solution preparation at approximately 97.36% because of the preparation of
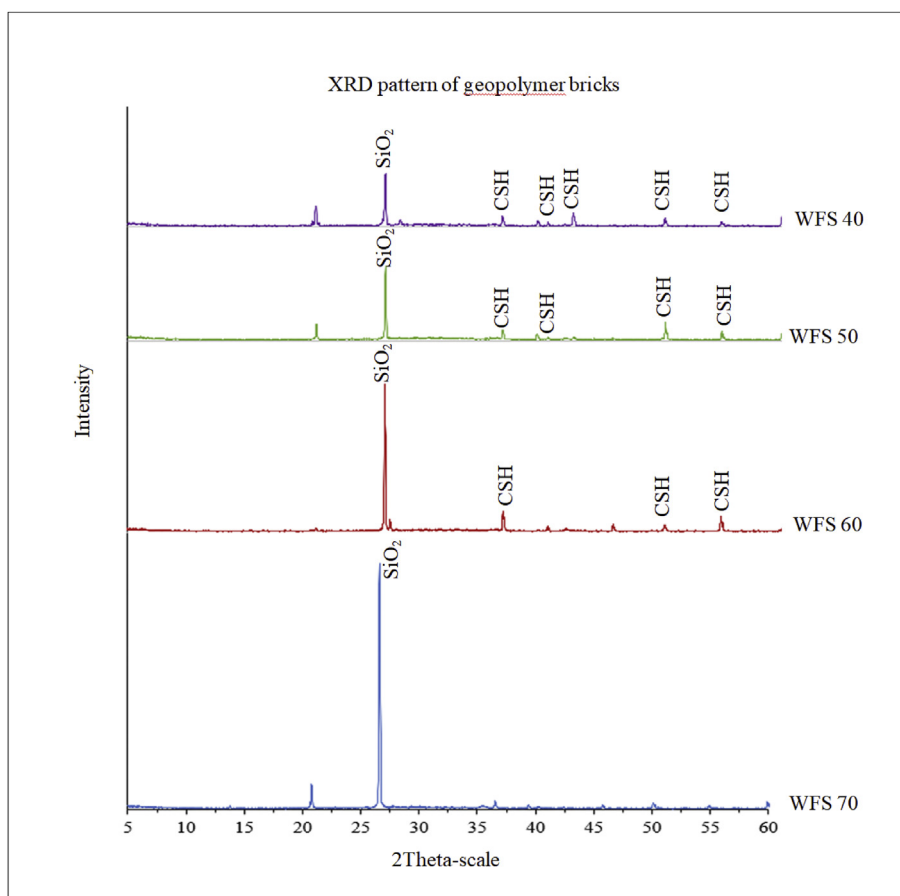
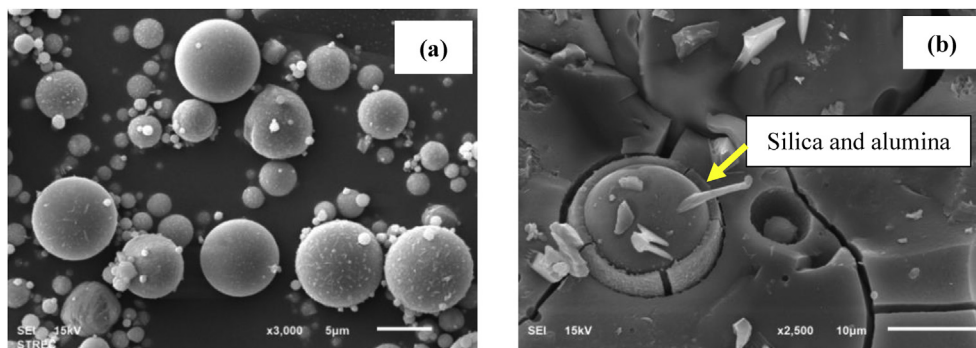**Figure 7.** *X-ray diffraction patterns of geopolymer brick.*

Figure 8. *The microstructures of (a) origin FA and (b) FA after reacted with alkaline solution.*

sodium hydroxide and sodium silicate. Moreover, the fume hood's electricity use can have an ozone depletion effect.

The main factor involved in terrestrial acidification, human toxicity, and terrestrial ecotoxicity was alkaline solution preparation at 46.04%, 80.84%, and 89.02%, respectively. The fume hood equipment's electricity use and the preparation of sodium hydroxide and sodium silicate contributed to this impact. The material preparation process also contributed to these categories due to the transportation of raw materials and the grinding and sieving machines.

The main factor related to fossil fuel depletion was the material preparation process (71.86%), followed by transportation (10.32%) and disposal in a landfill (10.32%). These three processes contributed to fossil fuel depletion through the combustion of diesel oil and the electricity used by the grinding and sieving machines.

3.3.2. Comparison of environmental impact categories for geopolymer bricks and concrete production

The environmental impact results of geopolymer brick production and of concrete production are presented in Table 6, and the summary of all categories is presented as a graph with a 100% total in Figure 11.

Geopolymer bricks made from 40% WFS, 30% FA, and 30% EAF were compared with concrete bricks (*Quebec and **North American) with a 25 MPa compressive strength. The results showed that the effects on climate change, ozone depletion, terrestrial acidification, human toxicity, terrestrial ecotoxicity, and fossil fuel depletion of geopolymer bricks were less than the effects of concrete bricks, as shown in Table 6.

The comparison was made between 1 m^3 of geopolymer bricks with a WFS: FA: EAF ratio of 40:30:30 cured at an ambient temperature and 1 m^3 of Quebec and North America concrete bricks. The results of the
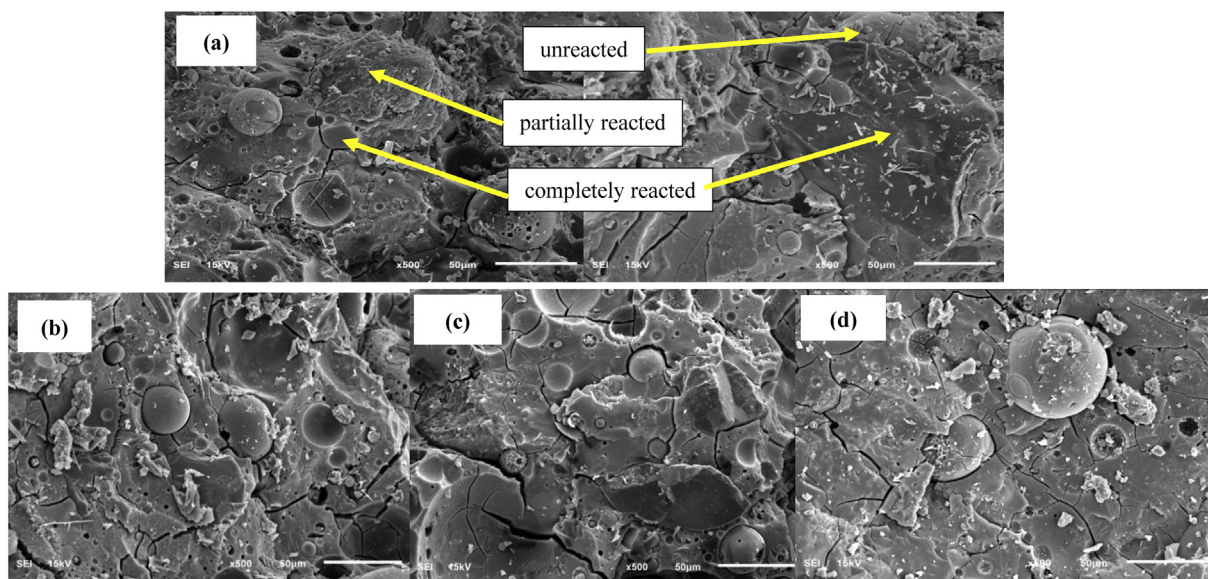
Figure 9. *The microstructure of (a) WFS70, (b) WFS60, (c) WFS50, and (d) WFS40.*

Table 5. *The leaching of heavy metals from WFS40.*

Heavy metal	WFS40 (mg/L)	TCLP limit (mg/L)
As	0.9620	5.0
Cr	0.0180	5.0
Cu	0.0050	Not given
Mn	0.2080	Not given
Pb	<0.005	5.0
Zn	0.5350	Not given

environmental impacts showed that emissions from geopolymer bricks were lower than North America concrete and Quebec concrete, respectively.

The emissions between geopolymer production and ordinary Portland cement (OPC) production were studied (Duxson et al., 2007). The results showed that the emission of geopolymer bricks was lower than that of OPC due to the calcination of the cement clinker in OPC that required a large amount of energy.

The literature review has presented the comparison between geopolymer bricks and concrete bricks, as showed in Figure 11. Both types of concrete bricks have different environmental impacts due to the amount of cement. North American concrete consumed 204 kg of cement, and Quebec concrete consumed 237 kg of cement; thus, Quebec concrete used more energy consumption in the calcination of the cement clinker than North America concrete. It can be concluded that concrete from North America is lower than that of Quebec concrete in all environmental impact categories.

Similarly, geopolymer bricks have the lowest environmental impact values compared with both types of concrete bricks due to no use of cement during production.
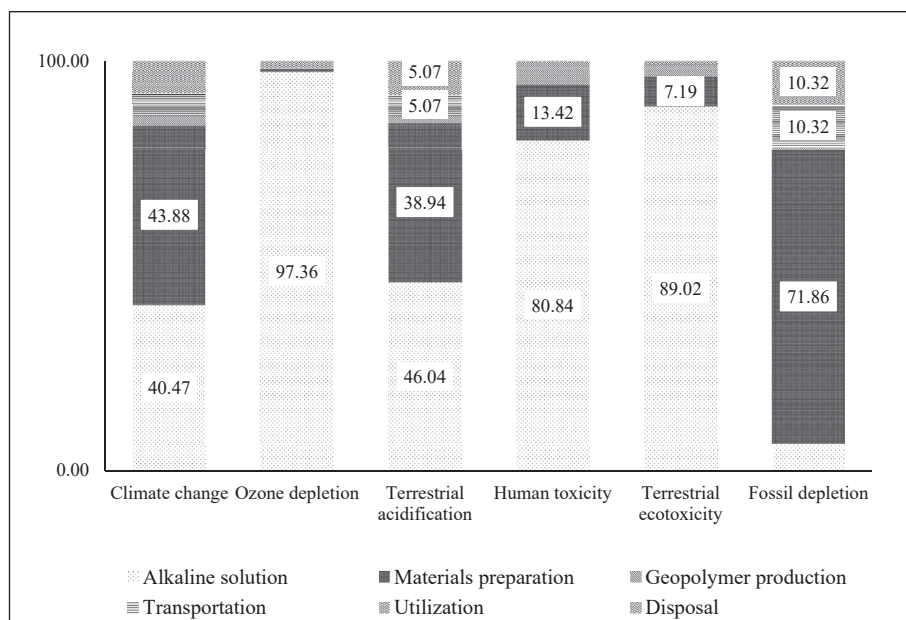

**Figure 10.** *Environmental impacts assessment for geopolymer bricks.*

Table 6. *Life cycle impact category for geopolymer bricks and concrete productions.*

Impact category	Geopolymer brick (25 MPa)	Concrete production* (25 MPa)	Concrete production** (25 MPa)
Climate change (kg CO_2 eq)	1.41	100	59.6
Ozone depletion (kg CFC-11 eq)	7.00	100	74.7
Terrestrial acidification (kg SO_2 eq)	2.87	100	62.8
Human toxicity (kg 1,4-DB eq)	2.96	100	71.3
Terrestrial ecotoxicity (kg 1,4-DB eq)	1.38	100	79.3
Fossil depletion (kg oil eq)	22.7	100	71.5

*, ** Database from Eco-Invent on SimaPro.

* Concrete, 25MPa (CA-QC) | concrete production 25MPa, RNA only | Alloc Def, U (Quebec) composed of Cement 237 Kg, Water 164 Kg, Gravel 950 Kg, Sand 940 Kg and Fly ash 18 Kg.

** Concrete, 25MPa (RoW)| concrete production 25MPa, RNA only | Alloc Def, U (North America) composed of Cement 204 Kg, Water 160 Kg, Gravel 1009 Kg, Sand 925 Kg and Fly ash 36 Kg.
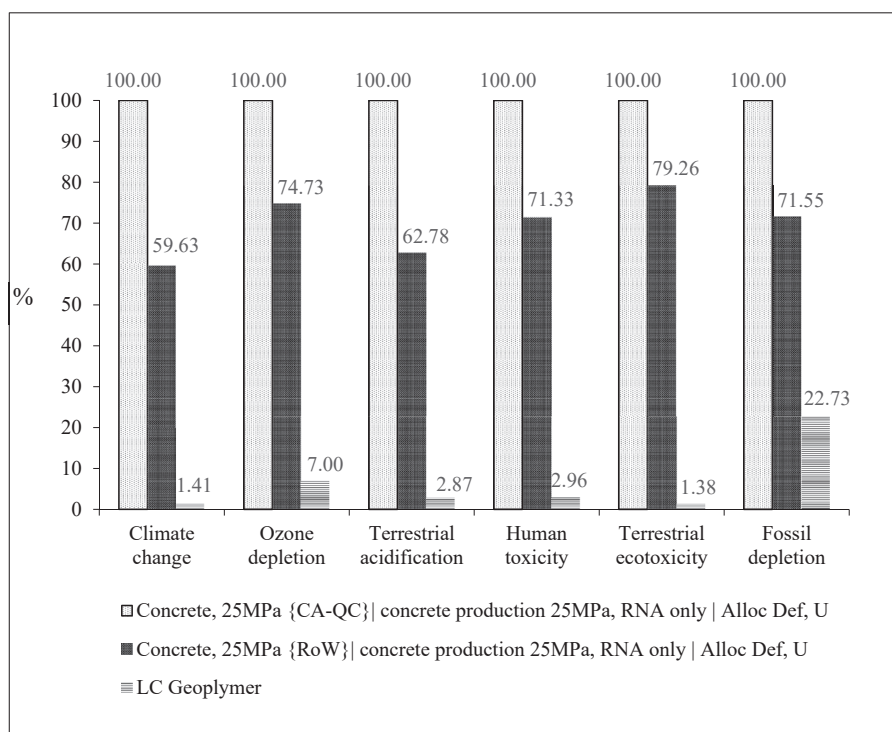
Figure 11. *Comparison of environmental impacts for geopolymer bricks and concrete bricks.*

4. Conclusions

This study focused on the potential use of industrial waste and industrial by-products to produce geopolymer bricks. This article has presented the results of an experiment investigating the use of WFS, FA, and EAF slag to produce geopolymer bricks. The geopolymerization process for WFS, FA, and EAF slag with an alkaline solution of $NaSiO_3/NaOH$ was successfully carried out to produce geopolymer bricks. The optimal ratio of WFS:FA:EAF to make geopolymer bricks, which was 40:30:30, was tested for the leaching of heavy metals using the TCLP method. Environmental impacts were assessed using LCA. Based on the experimental results, the following conclusions can be drawn:

1) The geopolymerization process of industrial waste, including WFS, FA, and EAF slag, was successfully carried out to produce geopolymer bricks after a curing time of 28 days at an ambient temperature. All sample ratios were higher than the compressive strength requirements of paving bricks (ASTM C902 1995) type II (>20.7 MPa) except WFS70.

2) The highest compressive strength was recorded at 25.76 MPa for geopolymer specimen WFS40, which was composed of 40% WFS, 30% FA, and 30% EAF slag.

3) The formation of CSH gels can be attributed to the increased proportion of EAF slag, the high CaO content of which reduces porosity and condenses the microstructure of a geopolymer mixture to enhance compressive strength.

4) Geopolymer brick can be classified as non-hazardous waste according to the acceptable leaching concentrations of heavy metals in the TCLP.

5) The LCA methodology was used to evaluate the environmental impact of geopolymer bricks from cradle to grave. The environmental impacts of geopolymer bricks depend on the manufacturing stage of the geopolymer. Almost all emissions may be attributed to energy consumption in the alkaline solution process and fuel consumption in the raw materials transportation process. The energy and fuel consumption of machines also produces a high amount of air pollutants, including CO_2, CH_4, N_2O, and SO_2.

6) The LCAs of 1 m³ of geopolymer brick with a WFS:FA:EAF ratio of 40:30:30 and of 1 m³ of Quebec and North American concrete brick

were compared. The results showed that emissions from the production of geopolymer bricks were lower than from the production of North American concrete and Quebec concrete due to the calcination of cement clinker during concrete production, which requires a large amount of energy.

Therefore, geopolymer bricks can be used to reduce industrial waste and add value to it as raw material to produce bricks using a more environmentally friendly production process.

Declarations

Author contribution statement

Suchanya Apithanyasai: Conceived and designed the experiments; Performed the experiments; Analyzed and interpreted the data; Wrote the paper.

Nuta Supakata: Conceived and designed the experiments; Analyzed and interpreted the data; Contributed reagents, materials, analysis tools or data; Wrote the paper.

Seksan Papong: Analyzed and interpreted the data; Contributed reagents, materials, analysis tools or data.

Funding statement

Competing interest statement

The authors declare no conflict of interest.

Additional information

No additional information is available for this paper.

Acknowledgements

References

Apithanyasai, S., Nooaek, P., Supakata, N., 2018. The utilization of concrete residue with electric arc furnace slag in the production of geopolymer bricks. J. Eng. 22, 1–14.

Arulrajah, A., Mohammadinia, A., Phummiphan, I., Horpibulsuk, S., Samingthong, W., 2016. Stabilization of recycled demolition aggregates by geopolymers comprising calcium carbide residue, fly ash and slag precursors. J. Construct. Build. Mater. 114, 864–873.

ASTM C902, 1995. Standard Specification for Pedestrian and Light Traffic Paving Brick.

ASTM C 109/C 109M, 2014. Standard Test Method for Compressive Strength of Hydraulic Cement Mortars (Using 2-in. Or [50-mm] Cube Specimens).

Chindaprasirt, P., Rattanasak, U., 2017. Characterization of the high-calcium fly ash geopolymer mortar with hot-weather curing systems for sustainable application. J. Adv. Powder Technol. 28 (9), 2317–2324.

Davidovits, J., Orlinski, J., 1988. Geopolymer' 88. European Conference on Soft Mineralurgy 1. Université de Technologie, Compiègne, France.

Duxson, P., Provis, J.L., Lukey, G.C., van Deventer, J.S.J., 2007. The role of inorganic polymer technology in the development of 'green concrete'. Cement Concr. Res. 37 (12), 1590–1597.

Electricity Generating Authority of Thailand, 2018. Utilization of lignite fly ash. accessed. http://maemoh.egat.com/index.php?option=com_content&view=article&id=89&Itemid=494. (Accessed 5 February 2019).

Fang, G., Bahrami, H., Zhang, M., 2018a. Mechanisms of autogenous shrinkage of alkali-activated fly ash-slag pastes cured at ambient temperature within 24 h. J. Construct. Build. Mater. 171, 377–387.

Fang, G., Ho, W.K., Tu, W., Zhang, M., 2018b. Workability and mechanical properties of alkali-activated fly ash-slag concrete cured at ambient temperature. J. Construct. Build. Mater. 172, 476–487.

Gürkan, E., Çoruh, S., Elevli, S., 2018. Adsorption of lead and copper using waste foundry sand: statistical evaluation. Int. J. Glob. Warming 14, 260–273.

Hadi, M.N.S., Al-Azzawi, M., Yu, T., 2018. Effects of fly ash characteristics and alkaline activator components on compressive strength of fly ash-based geopolymer mortar. J. Construct. Build. Mater. 175, 41–54.

Hazardous Substance and Environmental Management, 2015. Inventory Data of Recycle Waste. http://recycle.dpim.go.th/wastelist/download_files/G/waste_quantity.pdf. (Accessed 3 July 2019).

Huseien, G.F., Ismail, M., Tahir, M.M., Mirza, J., Khalid, N.H.A., Asaad, M.A., Husein, A.A., Sarbini, N.N., 2018. Synergism between palm oil fuel ash and slag: production of environmental-friendly alkali activated mortars with enhanced properties. J. Construct. Build. Mater. 170, 235–244.

Li, C., Sun, H., Li, L., 2010. A review: The comparison between alkali-activated slag (Si+Ca) and metakaolin (Si+Al) cements. Cement Concr. Res. 40, 1341–1349.

Phummiphan, I., Horpibulsuk, S., Rachan, R., Arulrajah, A., Shen, S.-L., Chindaprasirt, P., 2018. High calcium fly ash geopolymer stabilized lateritic soil and granulated blast furnace slag blends as a pavement base material. J. Hazard Mater. 341, 257–267.

Siddique, R., Kaur, G., Rajor, G., 2010. Waste foundry sand and its leachate characteristics. J. Resour., Conserv. Recycl. 54, 1027–1036.

Siddique, R., Noumowe, A., 2008. Utilization of spent foundry sand in controlled low-strength materials and concrete. Resour. Conserv. Recycl. 53 (1), 27–35.

Siddique, R., Singh, G., 2011. Utilization of waste foundry sand (WFS) in concrete manufacturing. Resour. Conserv. Recycl. 55, 855–892.

United States Environmental Protection Agency, 1992. Method 1311: Toxicity Characteristic Leaching Procedure. U.S, Cincinnati.

Yi, H., Xu, G., Cheng, H., Wang, J., Wan, Y., Chen, H., 2012. An overview of utilization of steel slag. Procedia Environ. Sci. 16, 791–801.

Zawrah, M.F., Gado, R.A., Feltin, N., Ducourtieux, S., Devoille, L., 2016. Recycling and utilization assessment of waste fired clay bricks (Grog) with granulated blast-furnace slag for geopolymer production. J. Process Saf. Environ. Prot. 103, 237–251.

Zhang, M., El-Korchi, T., Zhang, G., Liang, J., Tao, M., 2014. Synthesis factors affecting mechanical properties, microstructure, and chemical composition of red mud–fly ash based geopolymers. J. Fuel. 134, 315–325.

Zhang, M., Zhao, M., Zhang, G., Mann, D., Lumsden, K., Tao, M., 2016. Durability of red mud-fly ash based geopolymer and leaching behavior of heavy metals in sulfuric acid solutions and deionized water. J. Construct. Build. Mater. 124, 373–382.